

# Systematic Study of Triaxial Deformation in the Relativistic Mean Field Theory

S. Sugimoto<sup>a,b,1</sup>, K. Sumiyoshi<sup>a,2</sup>, D. Hirata<sup>a,c,3</sup>, B.V. Carlson<sup>d,4</sup>,  
I. Tanihata<sup>a,5</sup>, and H. Toki<sup>a,b,6</sup>

<sup>a</sup>The Institute of Physical and Chemical Research (RIKEN),  
Hirosawa, Wako, Saitama 351-0198, Japan

<sup>b</sup>Research Center for Nuclear Physics(RCNP), Osaka University,  
Mihogaoka, Ibaraki, Osaka 567-0047, Japan

<sup>c</sup>Japan Synchrotron Radiation Research Institute (JASRI) - SPring-8,  
Sayo, Hyogo, 679-5198, Japan

<sup>d</sup>Departamento de Física, Instituto Tecnológico da Aeronáutica - CTA,  
São José dos Campos, São Paulo, Brazil

---

<sup>1</sup>e-mail: satoru@postman.riken.go.jp

<sup>2</sup>e-mail: sumi@postman.riken.go.jp

<sup>3</sup>e-mail: daisy@sp8sun.spring8.or.jp

<sup>4</sup>e-mail: brett@fis.ita.cta.br

<sup>5</sup>e-mail: tanihata@rikaxp.riken.go.jp

<sup>6</sup>e-mail: toki@rcnp.osaka-u.ac.jp

## Abstract

We use the relativistic mean field (RMF) theory to systematically study the change of deformation of even-even nuclei in the proton-rich Xe region. We investigate the appearance of triaxial deformation in 25 nuclei in the region covering  $Z = 50 - 58$  and  $N = 64 - 72$  by performing constrained, triaxially symmetric RMF calculations of their energy surfaces. We include pairing correlations using the BCS formalism. We find that the Sn isotopes are spherical and the Te isotopes are very gamma unstable with shallow minima around  $\gamma = 60^\circ$ . Adding more protons, the Xe, Ba and Ce isotopes have prolate deformations with their sizes increasing with proton number. The neutron number dependence is found to be small. We compare the calculated results with the available experimental data on the binding energy and the radii.

# 1 Introduction

The recent progress of radioactive nuclear beam facilities has provided us with marvelous findings in nuclear physics. Exotic structures such as neutron halos [1] and neutron skins [2, 3] have been found in experimental studies of light unstable nuclei in the neutron-rich region. Much new information on the shapes and structures of nuclei far from stability is being revealed by the systematic measurement of radii and moments of unstable nuclei [4, 5]. Planned facilities in the world will access a large number of unstable nuclei in the whole region of the nuclear chart and enable us to explore where and how exotic phenomena of nuclear structure appear in the region far from the stability line [6, 7]. One of the great interests is to know where the deformation of unstable nuclei appears and how the shape of these nuclei changes along the isotopic and isotonic chains.

At the same time, the relativistic many-body framework has been extensively applied to study nuclei and nuclear matter [8, 9]. This has been motivated by the recent success of the relativistic Brueckner-Hartree-Fock (RBHF) theory, in which the strong density-dependent repulsion arises automatically from the relativistic many-body treatment, in reproducing the saturation property of nuclear matter [10, 11, 12]. Among other properties, the relativistic mean field (RMF) theory, which is the phenomenological framework of the RBHF theory, has been shown to be excellent at describing the properties of unstable nuclei as well as stable ones [13, 14, 15, 16, 17]. The RMF theory has also been successfully applied to the study of the deformation of nuclei, as well as other properties of the stable and unstable nuclei [18, 19, 20]. Furthermore, the RMF theory has been used to calculate the equation of state (EOS) of nuclear matter in the wide density and temperature regions tabulated for the application to supernova simulations [21]. Recently, a systematic study of all even-even nuclei up to the drip lines in the nuclear chart has been performed in the RMF theory with axial deformation [22]. The ground state properties of about 2000 even-even nuclei from  $Z = 8$  to  $Z = 120$  have been studied and all possible deformations of each nuclide have been surveyed using a constrained, axially deformed RMF model. Through the systematic analysis of the ground state deformations thus found, the pattern of the appearance of prolate and oblate deformations has been obtained. In the same study, it was also found that the coexistence of prolate and oblate shapes with

similar binding energies occurs in many nuclei in the nuclear chart. This coexistence suggests the possible appearance of deformation beyond the axial kind, such as triaxial or even higher order multipole deformations.

The appearance of triaxial deformation in this context has been studied in the case of the neutron-rich Sulfur isotopes [23]. In the axial RMF calculation for neutron-rich Sulfur isotopes, the energy curves as a function of the  $\beta$  deformation have two minima, at both prolate and oblate deformations, with energies very close to each other. Judging solely from the energy curve, one cannot conclude which ground state deformation is realized or whether yet another type of deformation appears. The RMF calculations with triaxial deformation of the same isotopes have been performed to clarify this point and a smooth shape transition from prolate to oblate shapes through triaxial shape has been found along the Sulfur isotopic chain [23]. This example motivates us to study further the appearance of triaxial deformation in other regions of the nuclear chart. It is interesting to explore where triaxial deformation appears in the nuclear chart, especially in relation with the behavior of the appearance of axial deformation.

In the present study, we have chosen to explore the proton-rich Xe region for the appearance of triaxial deformation. We have made a systematic study of 25 even-even nuclei covering  $Z = 50 - 58$  and  $N = 64 - 72$ , using the RMF theory with triaxial deformation, in order to clarify how their shapes change as a function of  $N$  and  $Z$  in this region. We have calculated the energy surface of those nuclei as a function of the deformation parameters,  $\beta$  and  $\gamma$ , to explore the ground state deformation. The previous study of  ${}_{54}\text{Xe}$ ,  ${}_{55}\text{Cs}$  and  ${}_{56}\text{Ba}$  isotopes using the RMF theory with axial deformation [24] was successful in reproducing the general features of the ground state properties. However, disagreement with the measured isotope shift for the proton-rich region, which might be due to triaxial deformation, was observed. In the systematic RMF calculation with axial deformation [22], which we will discuss in Sect. 3, the shape change from oblate to prolate shape occurs as  $Z$  increases, in a region in which the two shapes coexist. Thus, the axially symmetric RMF calculations strongly suggest that this region could contain triaxial deformed nuclei.

This region has been discussed as a possible region for triaxial deformation in studies using conventional frameworks [25, 26, 27, 28]. There have also been experimental efforts to measure

excitation energies in order to study the collective nature of the nuclei in this region [29, 30]. Studies of triaxial deformation within the mean field approach have also been performed in other regions of the nuclear chart [31, 32, 33, 34].

In Sect. 2, we describe the framework of the RMF theory with deformation. We discuss the behavior of the shape within the RMF theory under the assumption of axial symmetry in Sect. 3. We present the results of the calculations in the RMF theory with triaxial deformation in Sect. 4. Results of the calculations are discussed in Sect. 5. We summarize the paper in Sect. 6.

## 2 Relativistic mean field theory

We briefly describe the framework of the RMF theory and the procedure of the calculation. All details can be found in [8, 14, 23]. In the RMF theory, the system of nucleons is described by fields of mesons and nucleons under the mean field approximation. We start with the effective lagrangian, which is relativistically covariant, composed of meson and nucleon fields. We adopt a lagrangian with non-linear  $\sigma$  and  $\omega$  terms [35],

$$\begin{aligned} \mathcal{L}_{RMF} = & \bar{\psi} \left[ i\gamma_\mu \partial^\mu - M - g_\sigma \sigma - g_\omega \gamma_\mu \omega^\mu - g_\rho \gamma_\mu \tau_a \rho^{a\mu} - e\gamma_\mu \frac{1 - \tau_3}{2} A^\mu \right] \psi \\ & + \frac{1}{2} \partial_\mu \sigma \partial^\mu \sigma - \frac{1}{2} m_\sigma^2 \sigma^2 - \frac{1}{3} g_2 \sigma^3 - \frac{1}{4} g_3 \sigma^4 \\ & - \frac{1}{4} W_{\mu\nu} W^{\mu\nu} + \frac{1}{2} m_\omega^2 \omega_\mu \omega^\mu + \frac{1}{4} c_3 (\omega_\mu \omega^\mu)^2 \\ & - \frac{1}{4} R_{\mu\nu}^a R^{a\mu\nu} + \frac{1}{2} m_\rho^2 \rho_\mu^a \rho^{a\mu} - \frac{1}{4} F_{\mu\nu} F^{\mu\nu}, \end{aligned} \quad (1)$$

where the notation follows the standard one. On top of the Walecka  $\sigma$  -  $\omega$  model with photons and isovector-vector  $\rho$  mesons, non-linear  $\sigma$  meson terms are introduced to reproduce the properties of nuclei quantitatively and give a reasonable value for the incompressibility [36]. The inclusion of the non-linear term of  $\omega$  meson [37] is motivated by the recent success of the relativistic Brueckner-Hartree-Fock theory [10, 35]. Deriving the Euler-Lagrange equations from the lagrangian under the mean field approximation, we obtain the Dirac equation for the nucleons and Klein-Gordon equations for the mesons. The self-consistent Dirac equation and Klein-Gordon equations are solved by expanding the fields in terms of harmonic-oscillator wave functions [14, 23].

The RMF model contains the meson masses, the meson-nucleon coupling constants and the meson self-coupling constants as free parameters. We adopt the parameter set TMA, which was determined by fitting the experimental data of masses and charge radii of nuclei in a wide mass range [22, 38, 39]. The parameters are listed in Table 1. We remark that this parameter set has a mass dependence so as to reproduce nuclear properties quantitatively from the light mass region to the superheavy region. With the TMA parameter set, the symmetry energy is 30.68 MeV and the incompressibility is 318 MeV. Note that the bulk properties of nuclear matter at saturation with the parameter set TMA is calculated for uniform matter in the limit of infinite mass number.

The TMA parameter set has been used for the systematic study of all even-even nuclei up to the drip lines in the nuclear chart within the RMF framework under the assumption of axial symmetry [22]. It has been shown that the overall agreement of the calculated results using TMA with the experimental data of masses and charge radii is excellent and is found to be much better than the results of spherical RMF calculations with TMA. In the present study, we extend the RMF calculation with the TMA parameter set from the axially symmetric to the triaxially symmetric one, in order to explore the appearance of triaxial deformation in the region in which axial deformations with similar binding energies coexist. We discuss the correspondence between the axial and triaxial RMF calculations in the subsequent section.

In order to take into account triaxial deformation, the fields are expanded in terms of the eigenfunctions of a triaxially deformed harmonic oscillator potential [23]. We perform calculations that constrain the quadrupole moments of the nucleon distribution, in order to survey the coexistence of multiple shapes and to identify the ground state deformation. We use a quadratic constraint to calculate a complete map of the energy surface as a function of the deformation [23, 40]. We take a basis of up to  $N = 12$  major shells of the harmonic oscillator wave functions. This is normally enough for the constrained calculations in this mass range [23]. We have performed calculations with  $N = 14$  major shells in the case of no-pairing and found that the energy surface does not change significantly for moderate deformation. We have also performed non-constrained calculations with pairing up to  $N = 16$  and the convergence was generally good with  $N = 12$ .

We take the pairing window as given by Gambhir et al. [14] as  $\varepsilon - \lambda \leq 2(41A^{-1/3})\text{MeV}$ . As for the pairing correlations, we perform the RMF calculations with triaxial symmetry using a BCS formalism [14]. Since we calculate the energy surface in the full  $\beta - \gamma$  range, we take the pairing interaction strength for a given nucleus as  $G = 23/A[\text{MeV}]$  for both protons and neutrons [42].

Although the BCS-type treatment has often been used in the RMF calculations, it would be preferable to incorporate the pairing correlations in the relativistic many body framework in a consistent manner. A study with the relativistic Hartree-Bogoliubov theory has been performed under the assumption of spherical symmetry [43]. A systematic study of nuclear deformation within such a relativistic many-body framework is currently being made [44].

### 3 Numerical results

Before we present the results of the RMF calculation with triaxial symmetry, we discuss the corresponding results of the RMF calculation with axial symmetry [22]. We examine the behavior of the calculated ground state properties of even-even nuclei in the proton-rich Xe region. We note here that the calculated properties of deformations as well as masses and radii in this region agree very well with the experimental data.

In the region of  $Z = 50 - 58$  and  $N = 64 - 72$ , roughly speaking, the deformation changes according to the proton number, with a few exceptions. The Sn isotopes ( $Z = 50$ ) are dominated by a spherical shape and the Te isotopes ( $Z = 52$ ) have, for the most part, an oblate shape. The Xe, Ba and Ce isotopes ( $Z = 54 - 58$ ) all have a prolate shape. We show the energy surfaces for Te and Xe isotopes as functions of  $\beta$  deformation (Fig. 1). The general trend shows a transition in shape from spherical, through oblate, to prolate as the proton number increases.

Furthermore, there is always more than one energy minimum and shape coexistence is generally observed [22] in this region of nuclides, as can be seen in Fig. 1. For each nucleus there is a corresponding second minimum which has the deformation parameter,  $\beta$ , of opposite sign to that of the absolute minimum. The energy difference between the absolute minimum and the second minimum is generally small in this region.

We next present the RMF calculations with triaxial deformation for 25 nuclei covering the range  $Z = 50 - 58$  and  $N = 64 - 72$ . We present the energy surfaces of these nuclei in the  $\beta$  and  $\gamma$  deformation parameter space, calculated using constraints on the two deformation parameters. Figure 2 displays the energy surfaces of the Sn, Te, Xe, Ba, Ce ( $Z = 50 - 58$ ) isotopes with  $N = 64 - 72$ , arranged in the form of the nuclear chart. The spacing of contours is 1 MeV in total energy in all figures. The energy minimum is marked by the black region, in which the energy difference is less than 1 MeV from its absolute minimum energy.

As for the Sn isotopes, the minima appear consistently at the spherical shape ( $\beta = 0$ ). The Te isotopes show a  $\gamma$ -soft character, having similar energies along the  $\gamma$  direction. Most of the Xe, Ba and Ce isotopes have minima at prolate deformation. In some cases ( $^{124}\text{Ba}$ ,  $^{128}\text{Ba}$ ,  $^{126}\text{Ce}$ ,  $^{128}\text{Ce}$  and  $^{130}\text{Ce}$ ), the region of the shallow minimum extends to quite large  $\gamma$  deformation. These results indicate that the triaxial shape is not stable in those nuclei, but the energy surfaces are very  $\gamma$  soft.

## 4 Discussion

We discuss here the influence of the pairing correlations and the effective interaction on the triaxial RMF calculations. Since the consistent calculation of pairing correlations with deformation within the relativistic many-body framework is still under development, we have performed the RMF calculations with pairing correlations in the BCS formalism, as a first study of the appearance of axial and triaxial deformation. We see here the effect of pairing correlations on the magnitude of the binding energy and the deformation by comparing the results of calculations with and without pairing. We show in Fig. 3 the energy surfaces in the  $\beta - \gamma$  plane of  $^{120}\text{Te}$ ,  $^{122}\text{Xe}$  and  $^{124}\text{Ba}$  without and with pairing correlations. The qualitative behavior of the two cases is very similar. Generally speaking, the magnitude of the  $\beta$  deformation is reduced by the pairing correlations. The energy minimum seen at finite  $\gamma$  deformation in  $^{124}\text{Ba}$  is washed out by the inclusion of the pairing correlations.

In Fig. 4 we show the proton deformation parameters  $\beta$  extracted from the RMF calculation with axial deformation. In the same figure we also show the experimental data obtained from the B(E2) values[45]. In this figure we see that our results compare well with experimental



data.

We also calculate the energy surface of  $^{124}\text{Ba}$  with alternative NL1 parameter set [13] of the RMF theory in order to test the dependence of triaxial deformation on the choice of the RMF parameter. In Fig. 5, we compare the energy surfaces obtained by using the TMA and NL1 parameter sets. A well-distinguished minimum is seen at prolate deformation for the case of the NL1 parameter set. This feature is slightly stronger than in the TMA case. We mention that triaxial deformation is not found in calculations within the Skyrme-Hartree-Fock(SHF) theory[41]. It would be interesting to compare the energy surfaces of RMF and SHF theories in a wide mass range.

In Fig. 6 we show the total binding energy of the nuclei studied. The theoretical values are taken from the axially symmetric calculations, since no distinguished triaxial shapes were found in the triaxial calculations. We see slightly over binding for the Sn isotopes, which may be due to the use of the constant pairing correlations and will be studied further. We show in Fig. 7 the charge radius as a function of the neutron number. The general tendency is found to be quite satisfactory.

## 5 Summary

We have studied systematically the triaxial deformation of 25 even-even nuclei in the proton-rich Xe region. We have calculated their ground state structures in the RMF theory with triaxial deformation and with pairing correlations and obtained their energy surfaces in the plane of the deformation parameters,  $\beta$  and  $\gamma$ , by constraining the quadrupole moments. We have explored the appearance of triaxial deformation in the region covering  $Z = 50 - 58$  and  $N = 64 - 72$ , by looking for the minima of the derived energy surfaces in the triaxial deformation parameter space. Through comparisons with the results obtained in the RMF calculations with axial symmetry, we have discussed the correspondence between the coexistence of axial shapes and the appearance of triaxial shapes.

We have found no distinguished energy minima at triaxial deformations. However, the energy surfaces are often very  $\gamma$  soft. This feature is caused by the pairing correlations since, when we remove the pairing correlations in the RMF calculations, we find well distinguished

triaxial deformation in this mass region. We have compared the energy surfaces of two parameter sets, the TMA and NL1 ones. The TMA parameter set provides more softness in the  $\gamma$  direction than the NL1 one provides. Comparisons of the binding energies and deformations with experimental data are, in general, quite satisfactory.

We note here that we have not worked out the angular momentum and particle number projection, which have already been developed in the non-relativistic approach. The restorations of these symmetries may change somewhat the results on the deformation, as has been discussed in the non-relativistic description of deformed nuclei. The relativistic approach to triaxial deformation is not yet at such a level of systematic study and these refinements have not been considered here. This is certainly a direction for future work.

## Acknowledgment

We would like to thank J. Meng for fruitful discussions. The entire calculation was performed on the Fujitsu VPP500/30 and VPP700E/128 supercomputer at RIKEN, Japan. K. S. would like to express special thanks to the Computing Facility of RIKEN for a special allocation of VPP500/30 computing time for the first stage of this study.

## References

- [1] I. Tanihata, H. Hamagaki, O. Hashimoto, Y. Shida, N. Yoshikawa, K. Sugimoto, O. Yamakawa, T. Kobayashi and N. Takahashi, *Phys. Rev. Lett.* **55** (1985) 2676.
- [2] I. Tanihata, D. Hirata, T. Kobayashi, S. Shimoura, K. Sugimoto and H. Toki, *Phys. Lett.* **B289** (1992) 261.
- [3] T. Suzuki, H. Geissel, O. Bochkarev, L. Chulkov, M. Golovkov, D. Hirata, H. Irnich, Z. Janas, H. Keller, T. Kobayashi, G. Kraus, G. Münzenberg, S. Neumaier, F. Nickel, A. Ozawa, A. Piechaczek, E. Roeckl, W. Schwab, K. Sümmerer, K. Yoshida, I. Tanihata, *Phys. Rev. Lett.* **75** (1995) 3241.

- [4] J. H. Hamilton, *Treatise on Heavy Ion Science*, ed. D. A. Bromley (Plenum, New York), **8** (1989) 3.
- [5] E. W. Otten, *Treatise on Heavy Ion Science*, ed. D. A. Bromley (Plenum, New York), **8** (1989) 517.
- [6] I. Tanihata, *Progress in Particle and Nuclear Physics* **35** (1995) 505
- [7] See for example, *Proceedings of the fourth International Conference on Radioactive Nuclear Beams*, Ohmiya, Japan, 1996, *Nucl. Phys.* **A616** (1997).
- [8] B. D. Serot and J. D. Walecka, *Adv. Nucl. Phys.* **16** (1986) 1.
- [9] B. D. Serot, *Rep. Prog. Phys.* **55** (1992) 1855.
- [10] R. Brockmann and R. Machleidt, *Phys. Rev.* **C42** (1990) 1965.
- [11] L. Engvik, M. Hjorth-Jensen, E. Osnes, G. Bao and E. Ostgaard, *Phys. Rev. Lett.* **73** (1994) 2650.
- [12] R. Brockmann and H. Toki, *Phys. Rev. Lett.* **B68** (1992) 3408.
- [13] P.-G. Reinhard, M. Rufa, J. Maruhn, W. Greiner and J. Friedrich, *Z. Phys.* **A323** (1986) 13.
- [14] Y. K. Gambhir, P. Ring and A. Thimet, *Ann. of Phys.* **198** (1990) 132.
- [15] D. Hirata, H. Toki, T. Watabe, I. Tanihata and B. V. Carlson, *Phys. Rev.* **C44** (1991) 1467.
- [16] K. Sumiyoshi, D. Hirata, H. Toki and H. Sagawa, *Nucl. Phys.* **A552** (1993) 437.
- [17] K. Pomorski, P. Ring, G.A. Lalazissis, A. Baran, Z. Lojewski, B. Nerlo-Pomorska and M. Warda, *Nucl. Phys.* **A624** (1997) 349.
- [18] M. M. Sharma and P. Ring, *Phys. Rev.* **C46** (1992) 1715.
- [19] D. Hirata, H. Toki, I. Tanihata and P. Ring, *Phys. Lett.* **B314** (1993) 168.

- [20] G. A. Lalazissis and M. M. Sharma, Nucl. Phys. **A586** (1995) 201.
- [21] H. Shen, H. Toki, K. Oyamatsu and K. Sumiyoshi, Prog. Theor. Phys. **100** (1998) 1013.
- [22] D. Hirata, K. Sumiyoshi, I. Tanihata, Y. Sugahara, T. Tachibana, and H. Toki, Nucl. Phys. **A616** (1997) 438; RIKEN Preprint No. RIKEN-AF-NF-268
- [23] D. Hirata, K. Sumiyoshi, B. V. Carlson, H. Toki and I. Tanihata, Nucl. Phys. **A609** (1996) 131.
- [24] D. Hirata, H. Toki and I. Tanihata, Nucl. Phys. **A589** (1995) 239.
- [25] R. F. Casten, P. von Brentano, K. Heyde, P. Van Isacker and J. Jolie, Nucl. Phys. **A439** (1985) 289.
- [26] R. Wyss, A. Granderath, W. Lieberz, R. Bengtsson, P. von Brentano, A. Dewald, A. Gelberg, A. Gizon, J. Gizon, S. Harrisopulos, A. Johnson, W. Nazarewicz, J. Nyberg and K. Schiffer, Nucl. Phys. **A505** (1989) 337.
- [27] A. Gelberg, D. Lieberz, P. von Brentano, I. Ragnarsson, P. B. Semmes and I. Wiedenhöver, Nucl. Phys. **A557** (1993) 439c.
- [28] U. Meyer, A. Faessler and S. B. Khadkikar, Nucl. Phys. **A624** (1997) 391.
- [29] A. Dewald, P. Sala, R. Wrzal, G. Böhm, D. Liebrez, G. Siems, R. Wirowski, K. O. Zell, A. Gelberg, P. von Brentano, P. Nolan, A. J. Kirwan, P. J. Bishop, R. Julin, A. Lampinen and J. Hattula, Nucl. Phys. **A545** (1992) 822.
- [30] P. Petkov, R. Krücken, A. Dewald, P. Sala, G. Böhm, J. Altmann, A. Gelberg, P. von Brentano, R.V. Jolos and W. Andrejtscheff, Nucl. Phys. **A568** (1994) 572.
- [31] P. Bonche, H. Flocard, P. H. Heenen, S. J. Krieger and M. S. Weiss, Nucl. Phys. **A443** (1985) 39.
- [32] W. Koepf and P. Ring, Phys. Lett. **B212** (1988) 397.
- [33] S. Aberg, H. Flocard and W. Nazarewicz, Annu. Rev. Nucl. Part. Sci. **40** (1990) 439 and references therein.

- [34] T. R. Werner, J. A. Sheikh, W. Nazarewicz, M. R. Strayer, A. S. Umar and M. Misu, Phys. Lett. **B333** (1994) 303.
- [35] Y. Sugahara and H. Toki, Nucl. Phys. **A579** (1994) 557.
- [36] J. Boguta and A. R. Bodmer, Nucl. Phys. **A292** (1977) 413.
- [37] A. R. Bodmer, Nucl. Phys. **A526** (1991) 703.
- [38] Y. Sugahara, Doctor thesis, Tokyo Metropolitan University (1995).
- [39] H. Toki, D. Hirata, Y. Sugahara, K. Sumiyoshi and I. Tanihata, Nucl. Phys. **A588** (1995) 357c.
- [40] H. Flocard, P. Quentin, A. K. Kerman and D. Vautherin, Nucl. Phys. **A203** (1973) 433.
- [41] N. Tajima, S. Takahara and N. Onishi, Nucl. Phys. **A603** (1996) 23.
- [42] L. S. Kisslinger and R. A. Sorensen, Mat. Fys. Medd. Dan. Vid. Selsk. **32** No. 9 (1960) 5.
- [43] J. Meng and P. Ring, Phys. Rev. Lett. **77** (1996) 3963.
- [44] D. Hirata and B. V. Carlson, ENAM98, ed. B. M. Sherrill, D. J. Morrissey and C. N. Davids (The American Institute of Physics) (1998) 527.
- [45] S. Raman, C. H. Malarkey, W. T. Milner, C. W. Nestor, Jr., and P. H. Stelson, At. Data Nucl. Data Tables **36** (1987) 1.
- [46] G. Audi and A.H. Wapstra, Nucl. Phys. **A595** (1995) 409.
- [47] H. De Vries, C. W. De Jager and C. De Vries, At. Data Nucl. Data Tables **36** (1987) 495.

**Table 1**

$m_N$ [MeV]	938.900
$m_\sigma$ [MeV]	519.151
$m_\omega$ [MeV]	781.950
$m_\rho$ [MeV]	768.100
$g_\sigma$	$10.055 + 3.050/A^{0.4}$
$g_\omega$	$12.842 + 3.191/A^{0.4}$
$g_\rho$	$3.800 + 4.644/A^{0.4}$
$g_2$	$-0.328 - 27.879/A^{0.4}$
$g_3$	$38.862 - 184.191/A^{0.4}$
$c_3$	$151.590 - 378.004/A^{0.4}$

## Figure captions

**Fig.1** The energy curve obtained in axial RMF calculations as a function of the deformation parameter,  $\beta$ , for the  $_{52}\text{Te}$  and  $_{54}\text{Xe}$  isotopes. Calculated points are connected by dashed curves to guide the eye. Note that the curves for  $^{122}\text{Te}$  and  $^{124}\text{Te}$  are shifted downward by 0.02 MeV to distinguish them from the other curves.

**Fig.2** The energy surface in the plane of deformation parameters,  $\beta$  and  $\gamma$ , calculated in the RMF theory with triaxial deformation for nuclei in the range of  $Z = 50 - 58$  and  $N = 64 - 72$ , arranged in the form of the nuclear chart. The energy difference between the contours is 1 MeV in total binding energy. The energy minimum is marked by the black region, in which the energy difference is less than 1 MeV.

**Fig.3** The energy surfaces obtained in the triaxial RMF calculation without and with pairing are shown for  $^{120}\text{Te}$ ,  $^{122}\text{Xe}$  and  $^{124}\text{Ba}$ . The energy difference between the contours is 1 MeV in total binding energy. The energy minimum is marked by the black region.

**Fig.4** The proton deformation parameter  $\beta$ , obtained from the RMF calculation with axial deformation, is shown as a function of the neutron number. The experimental data are extracted from Ref. [45].

**Fig.5** The energy surfaces obtained in the triaxial RMF calculation with the NL1 and TMA parameter sets are shown for  $^{124}\text{Ba}$ . The energy difference between the contours is 1 MeV in total binding energy. The energy minimum is marked by the black region.

**Fig.6** The total binding energy calculated using the RMF theory with axial deformation is shown as a function of the neutron number. The experimental data are extracted from Ref. [46].

**Fig.7** The charge radius calculated using the RMF theory with axial deformation is shown as a function of the neutron number. The experimental data are extracted from Ref. [47].

# $^{52}\text{Te}_N$

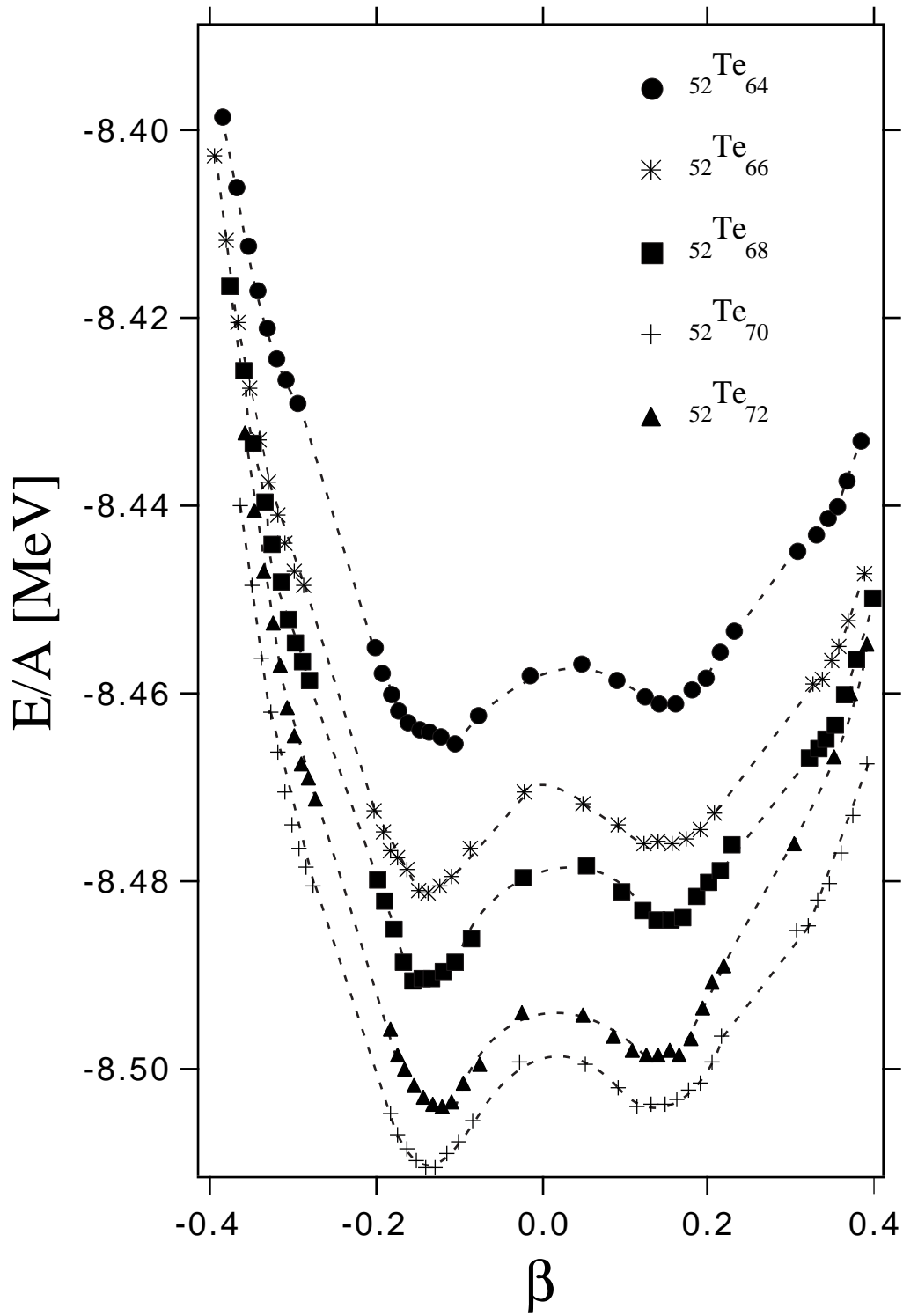


Figure 1a



$^{54}\text{Xe}_N$

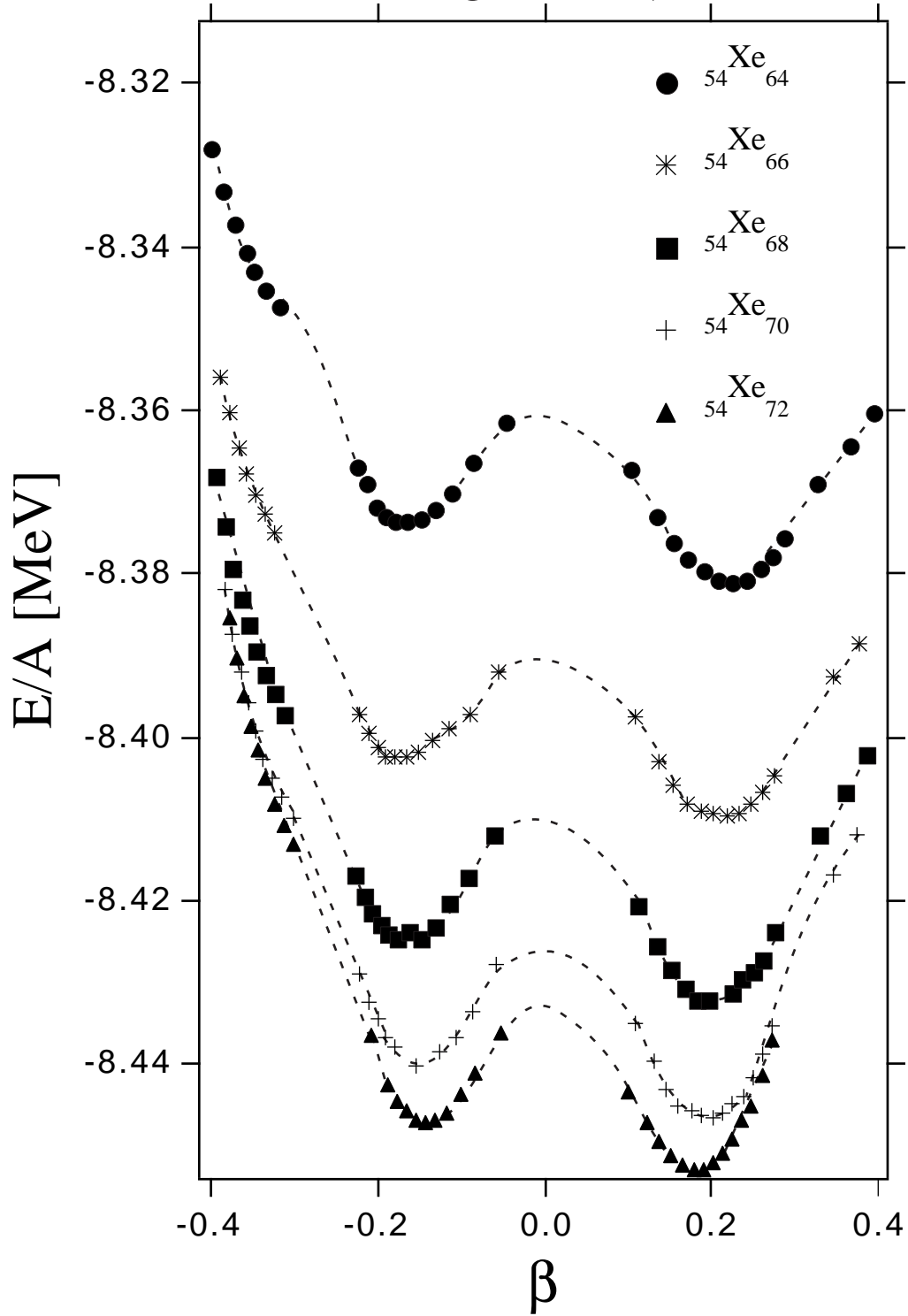


Figure 1b

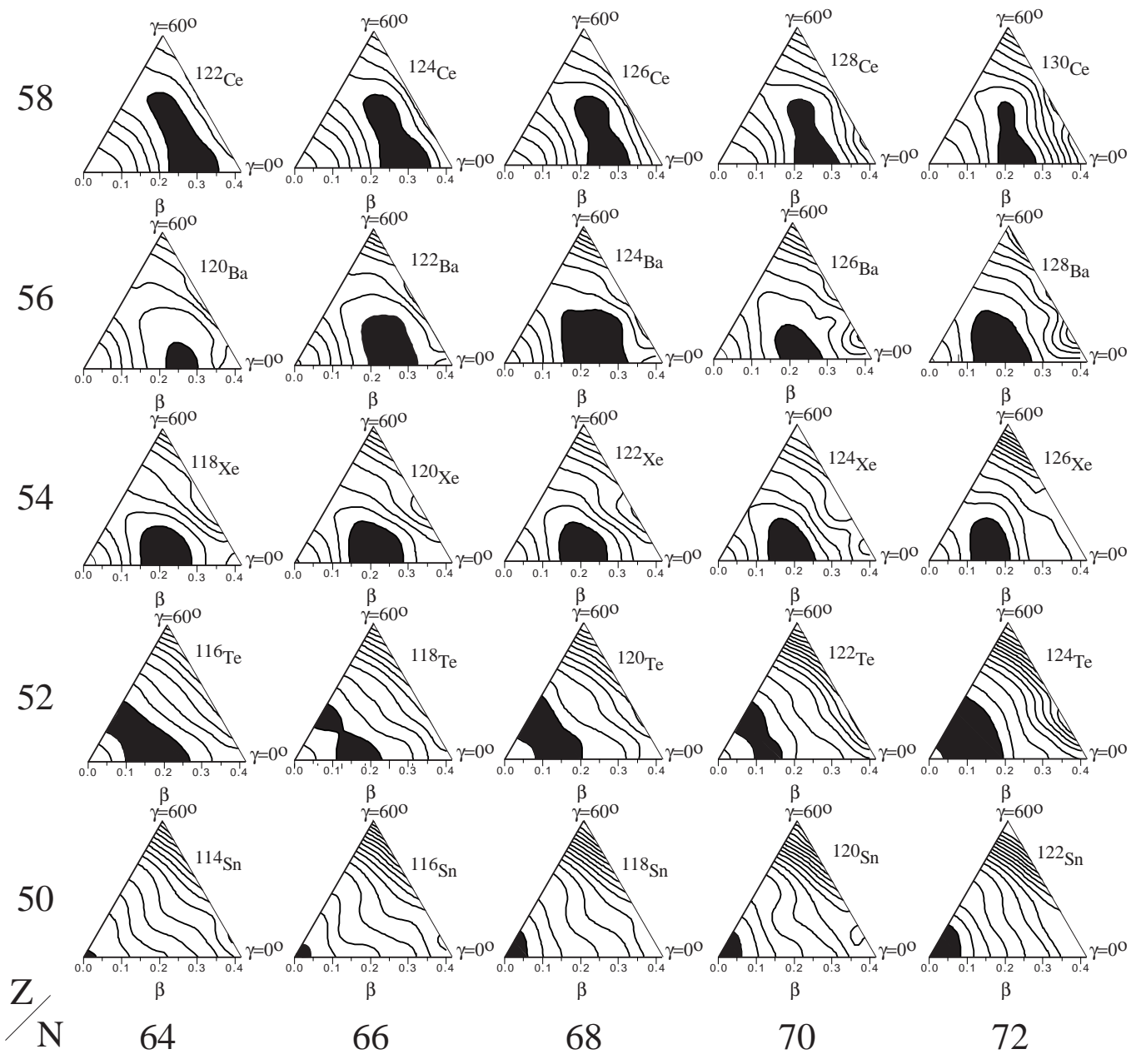
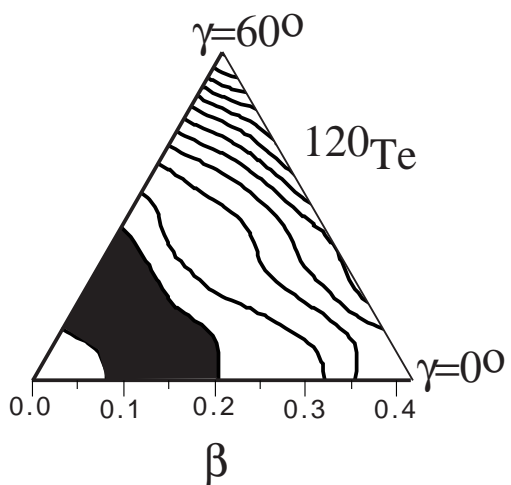
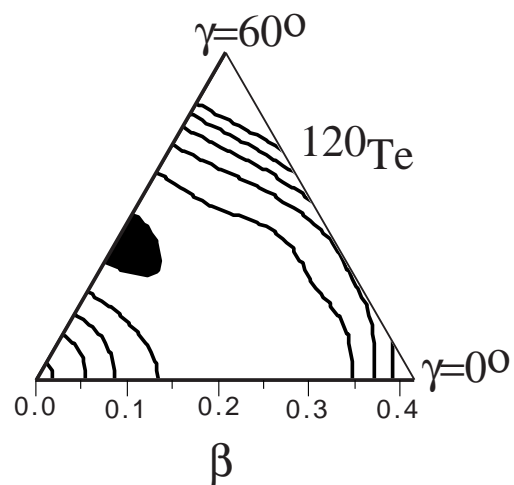
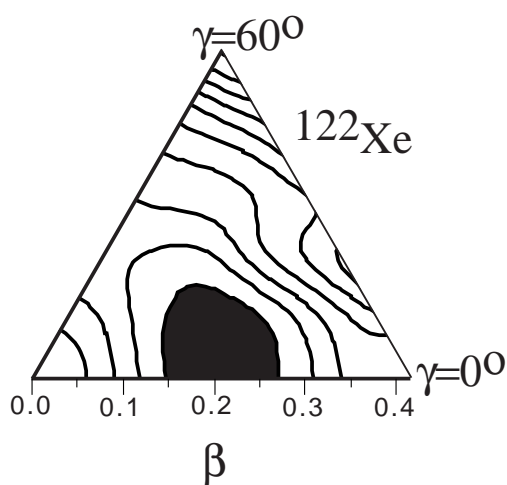
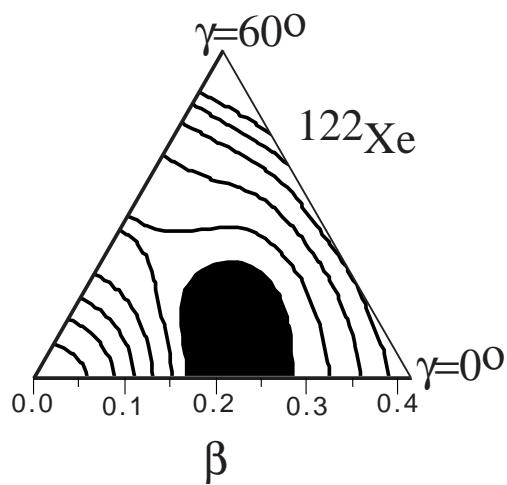
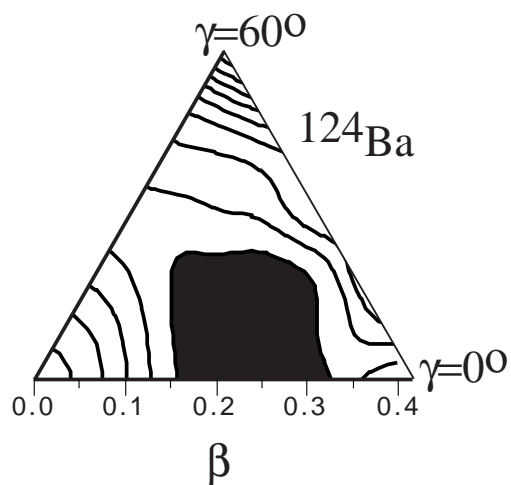
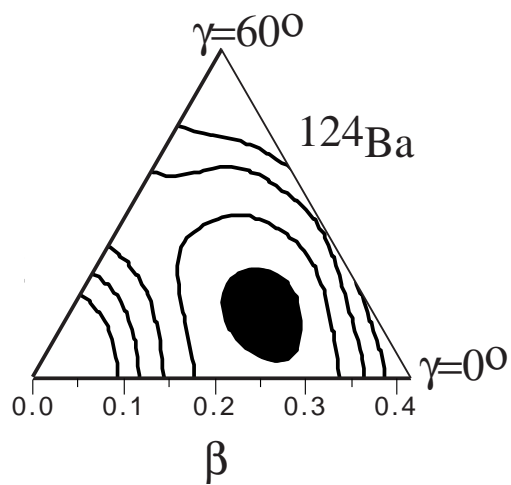


Figure 2



without pairing

with pairing

Figure 3

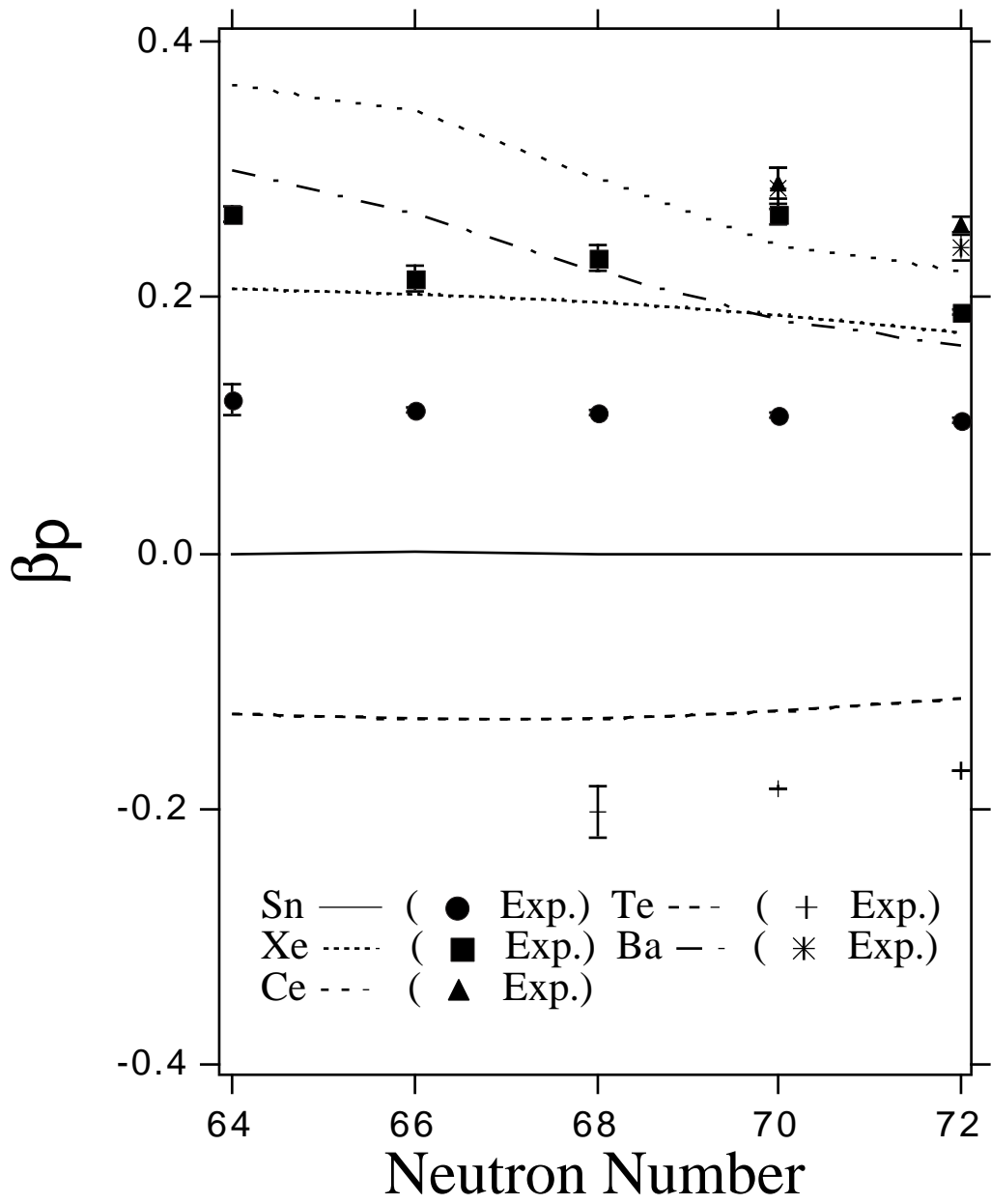


Figure 4

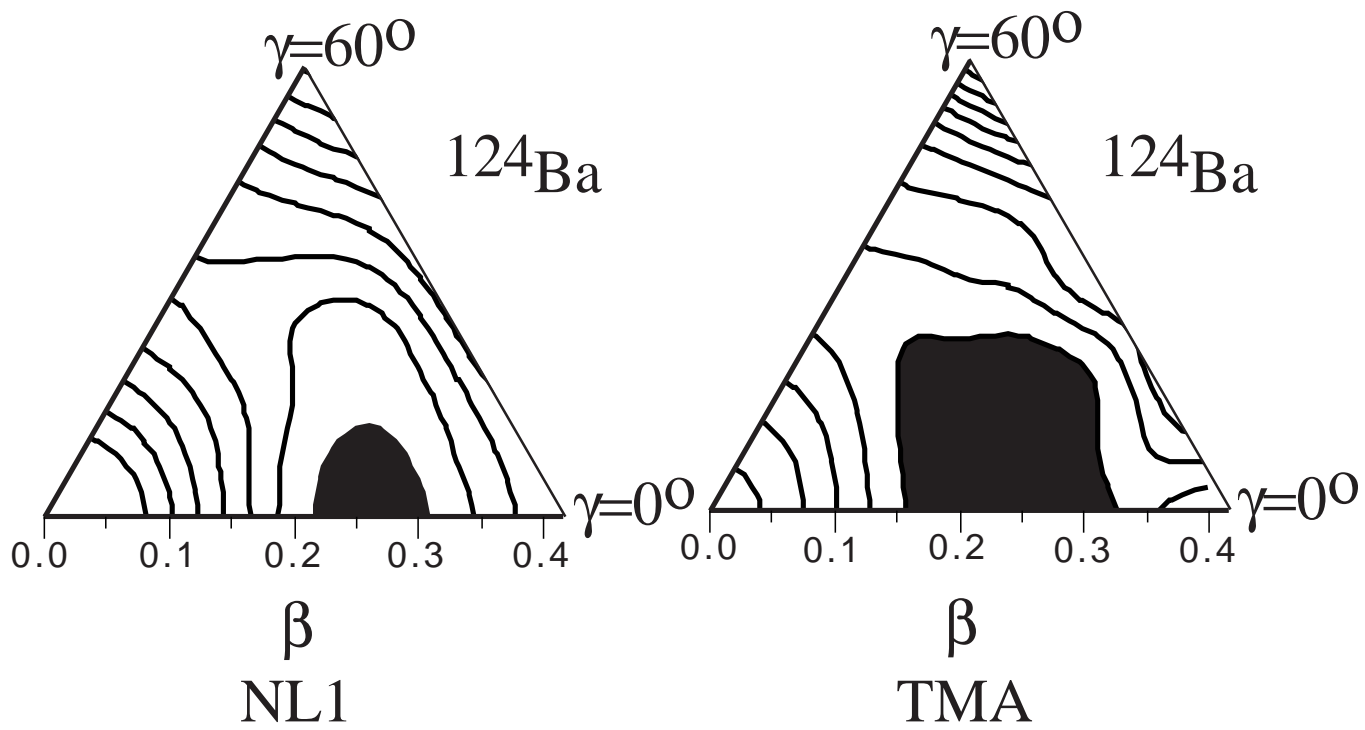


Figure 5

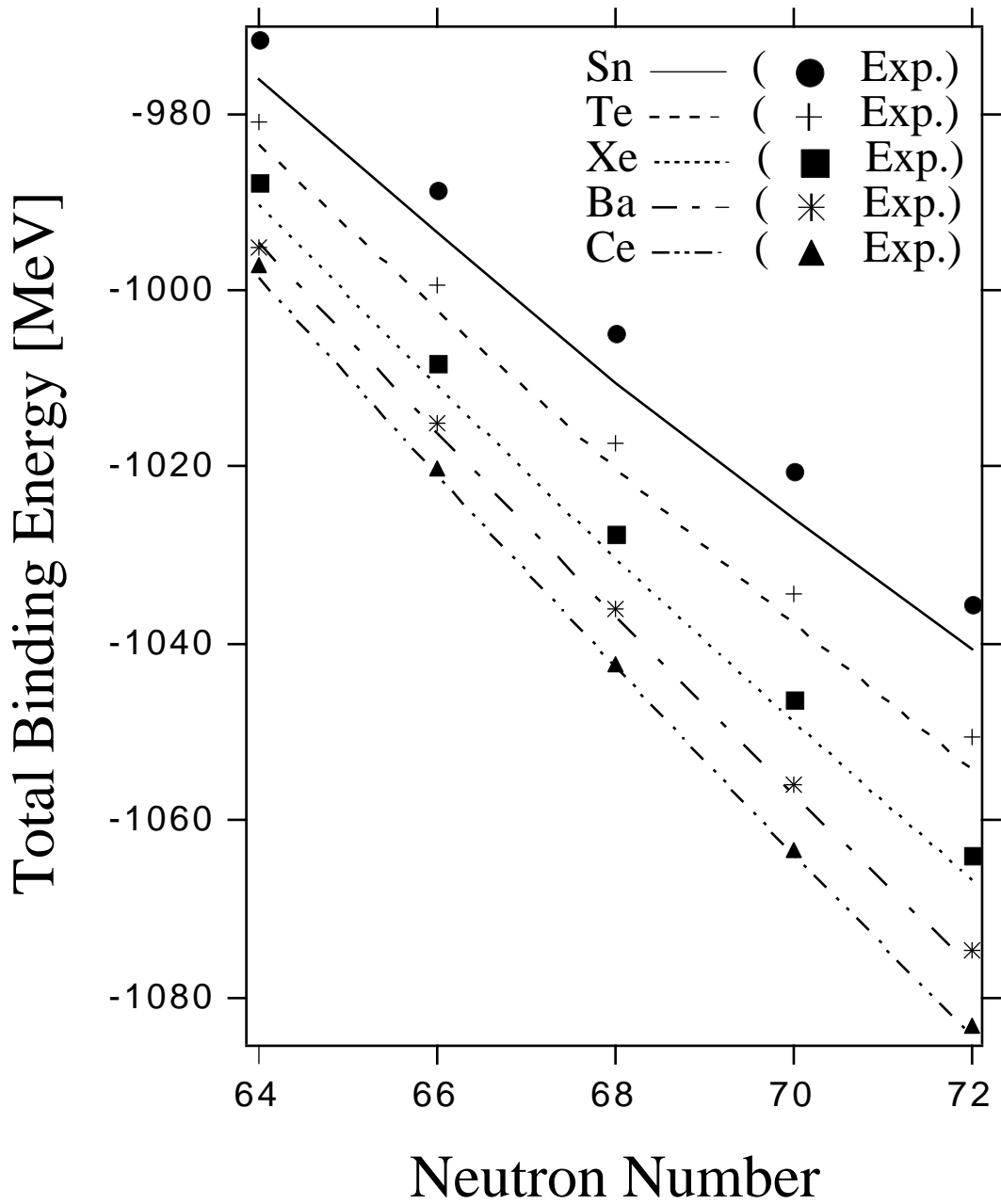


Figure 6

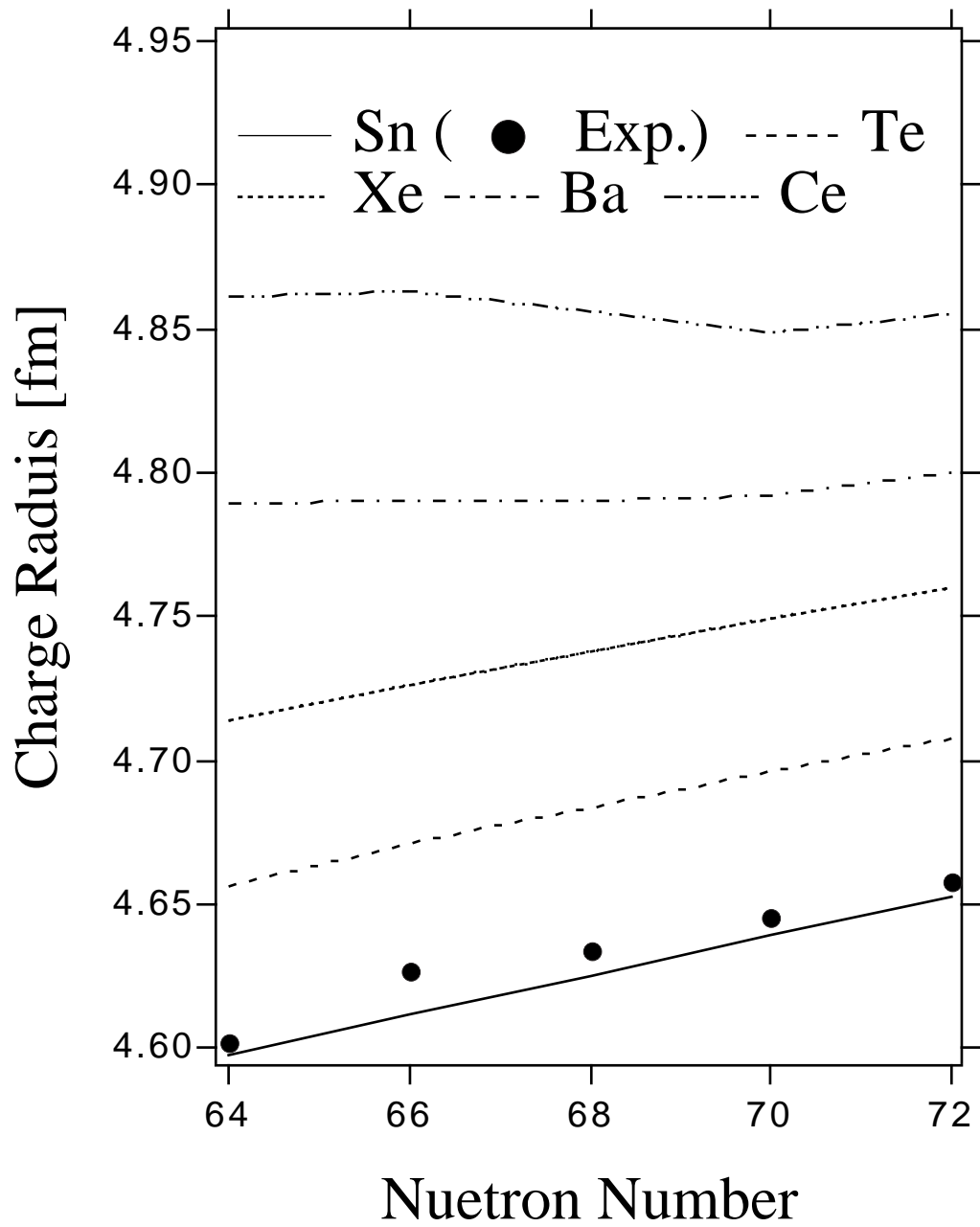


Figure 7